

Covalent and Selective Grafting of PEG Brushes at the Surface of ZIF-8 for the Processing of Membranes for Pervaporation.

Marvin Benzaqui,^{‡,||} Rocio Semino,^ζ Florent Carn,^φ Sergio Rodrigues Tavares,^ζ Nicolas Menguy,[⊥] Mónica Giménez-Marqués,^{‡,||} Elena Bellido,[‡] Patricia Horcajada,^{∘,‡} Thomas Berthelot,^Δ Anna I. Kuzminova,[§] Maria E. Dmitrenko,[§] Anastasia V. Penkova,[§] Denis Roizard,[#] Christian Serre,^{||,‡,*} Guillaume Maurin,^{ζ,*} Nathalie Steunou^{‡,*}

[‡]Institut Lavoisier de Versailles, UMR CNRS 8180, Université de Versailles St Quentin en Yvelines, Université Paris Saclay, 45 avenue des Etats-Unis 78035 Versailles Cedex. France.

^{||}Institut des Matériaux Poreux de Paris, FRE 2000 CNRS, Ecole Normale Supérieure, Ecole Supérieure de Physique et des Chimie Industrielles de Paris, PSL Research University, 75005 Paris, France.

^ζ Institut Charles Gerhardt Montpellier UMR 5253 CNRS, Université de Montpellier, Place E. Bataillon, 34095 Montpellier Cedex 05, France.

^φ Laboratoire Matière et Systèmes Complexes (MSC), UMR CNRS 7057, Université Paris Diderot, Bât. Condorcet, 10 rue A. Domon et L. Duquet, 75013 Paris, France.

[⊥] Sorbonne Université, UMR CNRS 7590, Muséum National d'Histoire Naturelle, IRD, Institut de Minéralogie, de Physique des Matériaux et de Cosmochimie, IMPMC, 75005 Paris, France.

[∘] Advanced Porous Materials Unit, IMDEA Energy, Av. Ramón de la Sagra 3, 28935 Móstoles, Madrid, Spain.

^Δ SPCSI Chemistry of Surfaces and Interfaces Group, CEA, IRAMIS F-91191, Gif-sur-Yvette, France.

[§] St. Petersburg State University, 7/9 Universitetskaya Nab., St. Petersburg 199034, Russia

[#] Laboratoire Réactions et Génie des Procédés, CNRS, Université de Lorraine, ENSIC, 1 rue Granville, 54000 Nancy, France.

* Corresponding authors :

christian.serre@ens.fr, Guillaume.Maurin@univ-montp2.fr, nathalie.steunou@uvsq.fr

(Summary of Content: 28 pages, 7 tables and 18 figures)

Table of Contents

I-Experimental Part and Methods	S2
1-Chemicals.....	S2
2-Synthesis of ZIF-8 NPs.....	S2
3-Synthesis of PEG-g-ZIF-8 NPs.....	S3
4-Characterization of ZIF-8 and of PEG-g- ZIF-8 NPs.....	S3
5-Preparation of colloidal suspensions of ZIF-8 and PEG-g-ZIF-8 NPs in PVA.....	S3
6-Characterization of colloidal suspensions of ZIF-8 and PEG-g-ZIF-8 NPs in PVA.....	S4
7-Preparation of dense PEG-g-ZIF-8/PVA membranes.....	S4
8-Preparation of supported PEG-g-ZIF-8/PVA membranes.....	S5
9-Characterization of PEG ₅₀₀₀ -g-ZIF-8/PVA membranes.....	S5
10-Pervaporation experiments.....	S5
II- Calculation of the PEG density on ZIF-8 surface.....	S6
III-Synthesis and Characterization of ZIF-8 and PEGylated ZIF-8 NPs.....	S8
IV-Characterization of Mixed Matrix Membranes based on PVA and ZIF-8 NPs.....	S14
V-Molecular modeling.....	S20
1-ZIF-8/PVA interface simulations.....	S20
2- PEG/PVA interface simulations.....	S24
VI- References.....	S25

I- Experimental part and Methods

1-Chemicals. All chemicals were used as received without further purification. $\text{Zn}(\text{NO}_3)_2 \cdot 6\text{H}_2\text{O}$ (99%), 4-Nitrobenzenediazonium tetrafluoroborate (97%), and Poly(ethylene glycol) methyl ether acrylate (noted Acryl-PEG480Da and Acryl-PEG5kDa) were purchased from Sigma Aldrich and 2-methylimidazole (Hmim) (97 %) from Alfa Aesar. Poly(vinyl alcohol) (PVA) is referenced as Mowiol® 20-98 with $M_w \approx 125\,000$ g/mol and with 98-98.8 mol% hydrolysis. Glutaraldehyde (GA) with a purity of >99.0% (abcr GmbH & Co. KG, Germany) was used. Isopropyl alcohol (i-PrOH) was obtained from “Vekton” (Russia). A hydrophilic porous support based on aromatic polysulfone amide (UPM, pore size 200Å, from Vladipor, Russia) was used to prepare supported membranes.

2-Synthesis of ZIF-8 NPs. ZIF-8 NPs were synthesized as previously reported by Tsai and Langner¹. A solution of $\text{Zn}(\text{NO}_3)_2 \cdot 6\text{H}_2\text{O}$ (2.933 g, 9.87 mmol) in 200 mL of MeOH is heated at 60 °C and then poured into a solution of Hmim (6.489 g, 79.04 mmol) in 200 mL of MeOH at 60 °C under stirring. After 1h, the milky solution is centrifuged at 14500 rpm for 15 min to recover ZIF-8 NPs which are then redispersed in 30 mL of methanol and centrifuged again twice to remove the excess of unreacted Hmim and zinc nitrate. The ZIF-8 NPs were washed

once again with 30 mL of H₂O. After final centrifugation, ZIF-8 NPs are redispersed and then stored in H₂O. ZIF-8 NPs are dried overnight at 100°C for further characterization by XRPD, TGA and FT-IR spectroscopy.

3-Synthesis of PEG-g-ZIF-8 NPs. A 10 g/L aqueous solution of ZIF-8 is prepared by dispersing 300 mg of ZIF-8 (on dry basis) in 30 mL of deionized H₂O. ZIF-8 solution is then sonicated using a US probe (2 min, 20 %) to obtain a good dispersion (solution A). A second solution is prepared by dissolving 360 mg of 4-nitrobenzenediazonium tetrafluoroborate in 30 mL of deionized H₂O. Acryl-PEG (0.225 g or 5.85 g for 5 kDa and 480 Da, respectively) is added to the diazonium salt solution and the mixture is stirred until the polymer is totally dissolved (solution B). Solutions A and B are then mixed and stirred for 1 min. The reducing agent, ascorbic acid (26 mg) was then introduced to initiate the reaction as confirmed by the formation of N₂ bubbles. The mixture is kept under stirring for 30 minutes at room temperature (RT). The dark red solution is then centrifuged and the liquid phase is discarded. The dark red product is then washed four times with 30 mL of absolute ethanol to remove the excess of diazonium salt. Then PEG-g-ZIF-8 is washed three times with deionized water to remove the excess of acryl-PEG. After removing the liquid phases, PEG-g-ZIF-8 is dispersed in H₂O. PEG-g-ZIF-8 samples are dried overnight at 100°C for further characterization by PXRD, TGA, N₂ sorption and FT-IR spectroscopy.

4-Characterization of ZIF-8 and PEG-g- ZIF-8 NPs. Samples were analyzed by FTIR (Nicolet 6700 FTIR spectrometer equipped with a DTGS detector) as self-supported wafers (ca. 15 mg). Spectra of the samples were recorded after heating at 200 °C for 5 hours under secondary vacuum ($\sim 10^{-3}$ Pa). X-ray powder diffraction patterns were collected using Siemens D5000 diffractometer ($\theta-2\theta$) with Cu radiation ($\lambda K_{\alpha} = 1.54059 \text{ \AA}$). BET surface areas of the materials were determined by N₂ adsorption in a BELSORP-Max porosimeter at 77 K. Prior to the analysis, ZIF-8 NPs were outgassed overnight under dynamic vacuum at 120 °C. Thermogravimetric analyses were performed on a Perkins Elmer SDA 6000 apparatus. Solids were heated up to 800 °C with a heating rate of 3 °C.min⁻¹ in an oxygen atmosphere.

5-Preparation of colloidal suspensions of ZIF-8 and PEG-g-ZIF-8 NPs in PVA. ZIF-8 and PEG-g-ZIF-8 solutions at [ZIF-8] concentrations (for PEG-g-ZIF-8, the weight concentration

is based on the amount of ZIF-8 and PEG) ranging from 0.1 to 1 g.L⁻¹ were prepared by diluting an initial 10 g.L⁻¹ aqueous stock solution with H₂O. ZIF-8 solutions were sonicated using a horn (20%; 1 min), before adding the desired amount of a 5 wt% aqueous solution of PVA. Colloidal dispersions of ZIF-8/PVA and PEG-g-ZIF-8/PVA with PVA/ZIF-8 weight ratio ranging from 0.5 to 0.9 were prepared. Before DLS measurements, each solution was stirred for several hours and sonicated (horn, 10%, 1 min).

6-Characterization of colloidal suspensions of ZIF-8 and PEG-g-ZIF-8 NPs in PVA. DLS measurements were performed on a Zetasizer from Malvern Instruments. ZIF-8 and ZIF-8/PVA solution with [ZIF-8] = 1 g.L⁻¹ were sonicated before DLS measurements. Solutions were analyzed in a glass cuvette with a 4 mW HeNe LASER operating at $\lambda = 632.8$ nm and a detection angle of 173°. The colloidal stability of ZIF-8/PVA solutions was evaluated by measuring the evolution of their diameter and polydispersity index (PDI) with time up to a total time of 9 minutes. The integration time per measurement point was 10 seconds. HRTEM images were recorded on a JEOL 2100F microscope operating at 200 kV, equipped with a Schottky emission gun, a high resolution UHR pole piece and a Gatan US4000 CCD camera. Samples were prepared by deposition of two droplets of colloidal suspensions onto a carbon-coated copper grid with a filter paper to absorb the excess of solution. STEM-HAADF experiments were performed using a JEOL annular detector. X-ray energy dispersive spectroscopy (XEDS) analyses were carried out using a Jeol detector with an ultrathin window allowing detection of light elements. SAXS experiments were performed at 25 ° C with samples placed in sealed quartz capillaries on SWING beamline (SOLEIL, Saint-Aubin, France) with a configuration $D = 2$ m and $\lambda = 1$ Å to get a q -range from 1.7×10^{-3} Å⁻¹ to 0.28 Å⁻¹.

7-Preparation of dense PEG-g-ZIF-8/PVA membranes. 2 wt.% aqueous PVA solution was prepared by dissolving a predetermined sample of PVA powder in distilled water at 85 °C during 5 hours with constant stirring. PVA solution was added in the same volume to a certain quantity of the PEG₅₀₀₀-g-ZIF-8 solution (20 g.L⁻¹). The obtained solution was kept in an ultrasonic bath for 2 hours and was mixed with the remaining amount of PVA solution followed by ultrasonication. Then the PEG₅₀₀₀-g-ZIF-8 (0, 5, 10, 15 wt.% with respect to PVA weight)/PVA solution was stirred for 24 hours. Membranes were finally cast from these solutions onto a Petri dish followed by the solvent evaporation. The introduction of PEG₅₀₀₀-g-ZIF-8 more than 15 wt.% into PVA matrix led to significant deterioration of the mechanical properties of membranes (membranes crumbled in the hands).

Cross-linked (CL) PEG-g-ZIF-8/PVA membranes were also prepared. According to the methodology previously reported,² the cross-linking procedure was carried out by adding a determined quantity of 25 wt.% glutaraldehyde (GA) aqueous solution and 36 wt.% hydrochloric acid to the PEG₅₀₀₀-g-ZIF-8 (0, 5, 10, 15 wt.%)/PVA solutions. The solutions were then stirred for 15 minutes. Membranes were finally cast from these solutions onto a Petri dish followed by the solvent evaporation.

8-Preparation of supported PEG-g-ZIF-8/PVA membranes. Supported membranes were prepared by casting 3 wt.% aqueous solution of PVA or the CL-PEG₅₀₀₀-g-ZIF-8/PVA (15 wt%) colloidal solution onto the surface of the commercial ultrafiltration porous UPM-20 support based on polysulfonamide, followed by drying at RT for 24 h for solvent evaporation.

9-Characterization of PEG₅₀₀₀-g-ZIF-8/PVA membranes. X-ray powder diffraction patterns were collected using Siemens D5000 diffractometer ($\theta-2\theta$) with Cu radiation ($\lambda K_{\alpha} = 1.54059$ Å). Cross-sections micrographs of the dense and supported membranes were recorded by using a Zeiss Merlin SEM equipment (observation at 1 kV). The samples were immersed into liquid nitrogen and fractured perpendicular to the surface. The contact angles of dense membranes were measured from both sides of the membranes by sessile drop method while for supported membranes it was carried out from the thin selective PVA layer.

The swelling degree of the dense membranes was studied by gravimetric method. Membranes of known weight were immersed in a weighing bottle with an azeotropic mixture iPrOH-water (12 wt.% of water) and weighed daily until a constant weight value. The equilibrium swelling degree S_0 (%) was calculated using the equation:

$S_0 = [(m_n - m_0) / m_0] \cdot 100$, where m_n is the weight of the swollen membrane, m_0 is the initial weight of the sample.

10-Pervaporation experiments. The pervaporation experiment was performed using a laboratory cell in steady state mode at various temperatures, the description of which was presented in the previous study.³ SHIMADZU GC-201 (Shimadzu, Kyoto, Japan) chromatograph was used for determination of the feed and permeate composition. The membrane flux J (kg/(m²h)) (membrane permeation flux), including the fluxes of both penetrating components: water and i-propanol,⁴ was calculated by the equation:

$$J = W/(A \cdot t),$$

where W (kg) is the weight of the liquid permeate (water and isopropanol), A (m²) is the membrane area, and t (h) is the time of the measurement. Each measurement was carried out at least three times to ensure a good accuracy of the transport parameters.

The stability of CL-PEG₅₀₀₀-g-ZIF-8/PVA (15 wt% MOF) membrane under pervaporation experiments was studied by carrying out the separation of IPA/H₂O (88:12 w/w) mixture at 25 °C during 7 days (see Figure 3(f)). The membrane was used for 12 hours for the IPA/H₂O (88:12 w/w) separation. Then, the feed was removed from the membrane and vacuum was stopped. The membrane was dried in the cell during the night. In the next day, the feed was poured to the pervaporation set-up and the separation was continued. This procedure was repeated during 7 cycles (days).

II- Calculation of the PEG density on ZIF-8 surface.

Calculations for M(PEG) = 5000 Da and radius = 12.5 nm and 10 wt% of PEG:

$$n(PEG) = \frac{m(PEG)}{M(PEG)} = \frac{0.1}{5000} = 2.10^{-5} mol = 20 \mu mol \quad \text{Equation S1}$$

$$\text{number of PEG chains} = n(PEG) \times N_A = 2.10^{-5} \times 6.022.10^{23} = 1.2.10^{19}$$

$$\begin{aligned} \text{number of NPs} &= \frac{\text{Total volume of MOF}}{\text{Volume of a sphere}} = \frac{\frac{\text{masse of ZIF8}}{\text{density of ZIF8}}}{\frac{4}{3}\pi r^3} = \frac{\frac{0.9}{0.92}}{\frac{4}{3}\pi(12.5)^3} \\ &= 1.195.10^{17} \end{aligned}$$

$$\text{number of chains per NPs} = \frac{n(PEG) \times N_A}{\text{nb of NPs}} = 100 \quad \text{Equation S2}$$

$$\text{PEG chains per nm}^2 = \frac{\text{nb of chains per NPs}}{\text{Ext surface area of ZIF - 8}} = \frac{100}{4\pi r^2} = \frac{100}{4\pi(12.5)^2} = 0.052$$

Therefore : $[\Gamma] = 5.2$ PEG molecules per 100 nm²

For 480 Da: 1049 chains per NPs and 53 chains per 100 nm² (x 10 compared to PEG 5kDa)

According to the papers of Auguste *et al*⁵ and Xu *et al*,⁶ full surface mushroom coverage ($[\Gamma^*]$) represents the number of unconstrained PEG molecules per 100 nm². To calculate $[\Gamma^*]$, we consider that PEG chains obey random-walk statistics and occupy an area at the interface given by a sphere of diameter ξ .

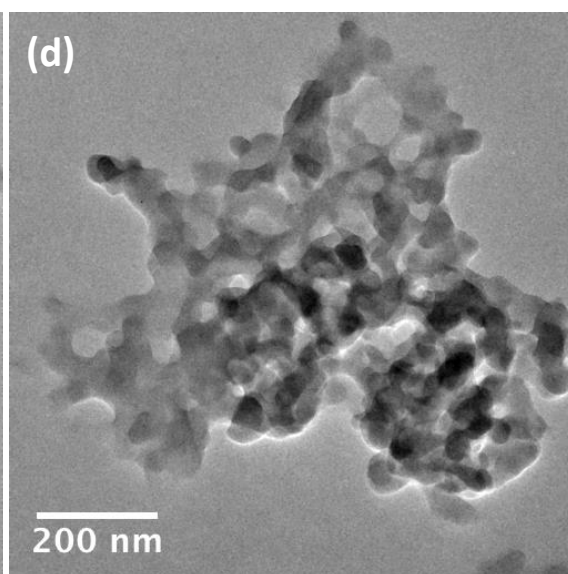
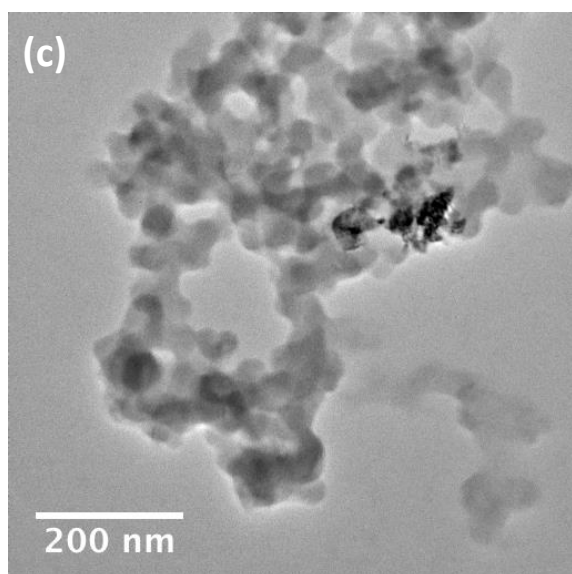
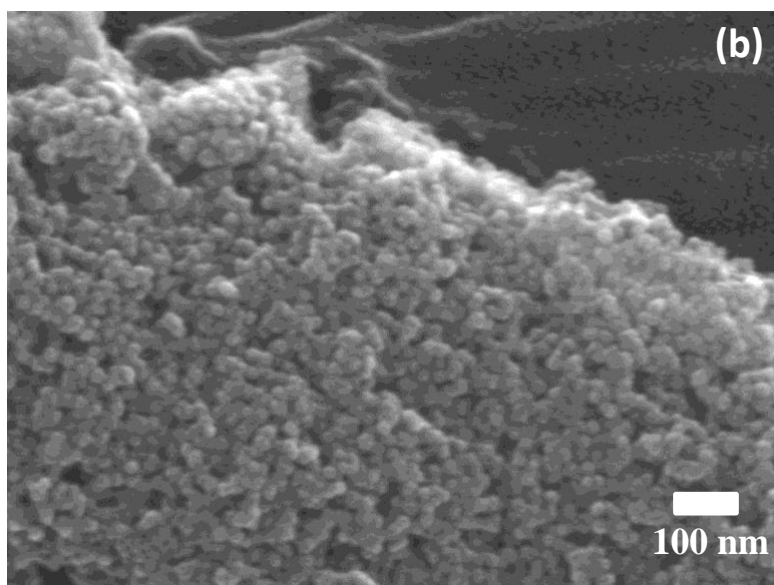
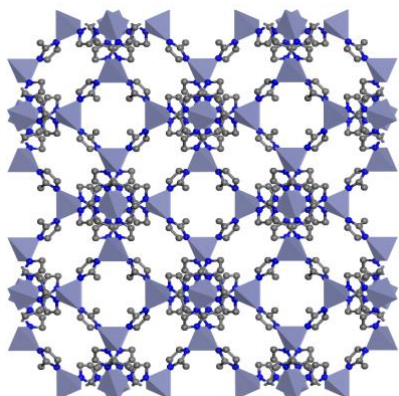
$$\xi = 0.76 M(PEG)^{0.5} [\text{\AA}] \quad \text{Equation S3}$$

The surface area occupied by one PEG molecule can be calculated by $\pi (\xi/2)^2$.

Thus PEG₅₀₀₀ and PEG₄₈₀ have an unconstrained molecule sphere with diameter of 5.4 and 1.7 nm respectively and occupy a surface area of 22.7 and 2.2 nm² respectively.

III-Synthesis and Characterization of ZIF-8 and PEGylated ZIF-8 NPs.

(a)



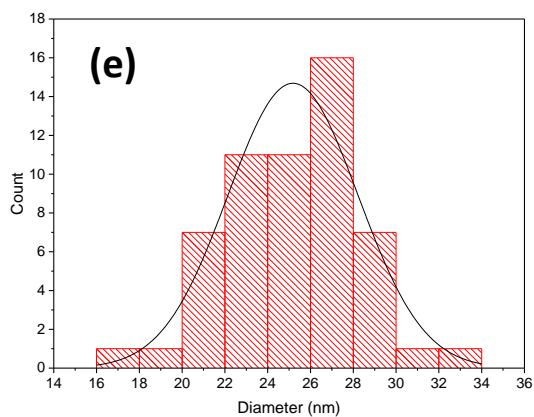


Figure S1. (a) Molecular structure of ZIF-8, (b) SEM image of ZIF-8 NPs, (c, d) TEM images of PEG₅₀₀₀-g-ZIF-8 NPs, (e) Size distribution of PEG₅₀₀₀-g-ZIF-8 NPs. Average diameter is 25±6 nm.

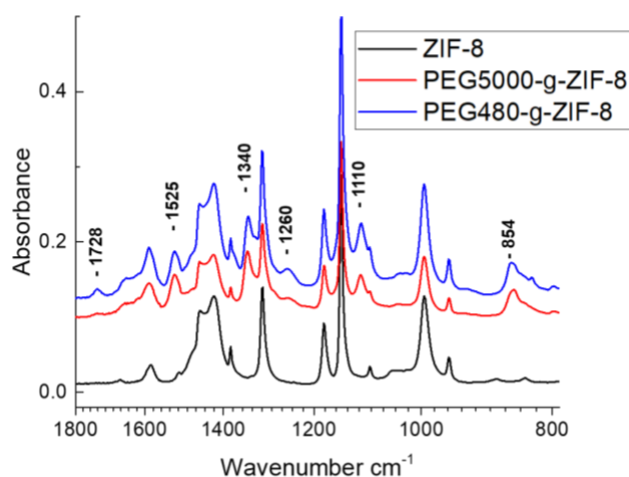


Figure S2. FT-IR spectra of ZIF-8 and PEG-g-ZIF-8 NPs showing additional peaks corresponding to PEG and nitrobenzene functional groups.

Table S1: Assignment of IR peaks for PEG-g-ZIF-8 NPs (480 Da and 5 kDa).

Wavenumber (cm ⁻¹)	Assignments	
1728	v(C=O)	Aliphatic ester (PEG)
1525	v(as)(N-O)	Ar-NO ₂
1340	v(s)(N-O)	Ar-NO ₂
1260	v(C-O)	Ether (PEG)
1110	v(C-O-C)	Ether (PEG)
854	v(C-C)	-(CH ₂ -CH ₂)- (PEG)

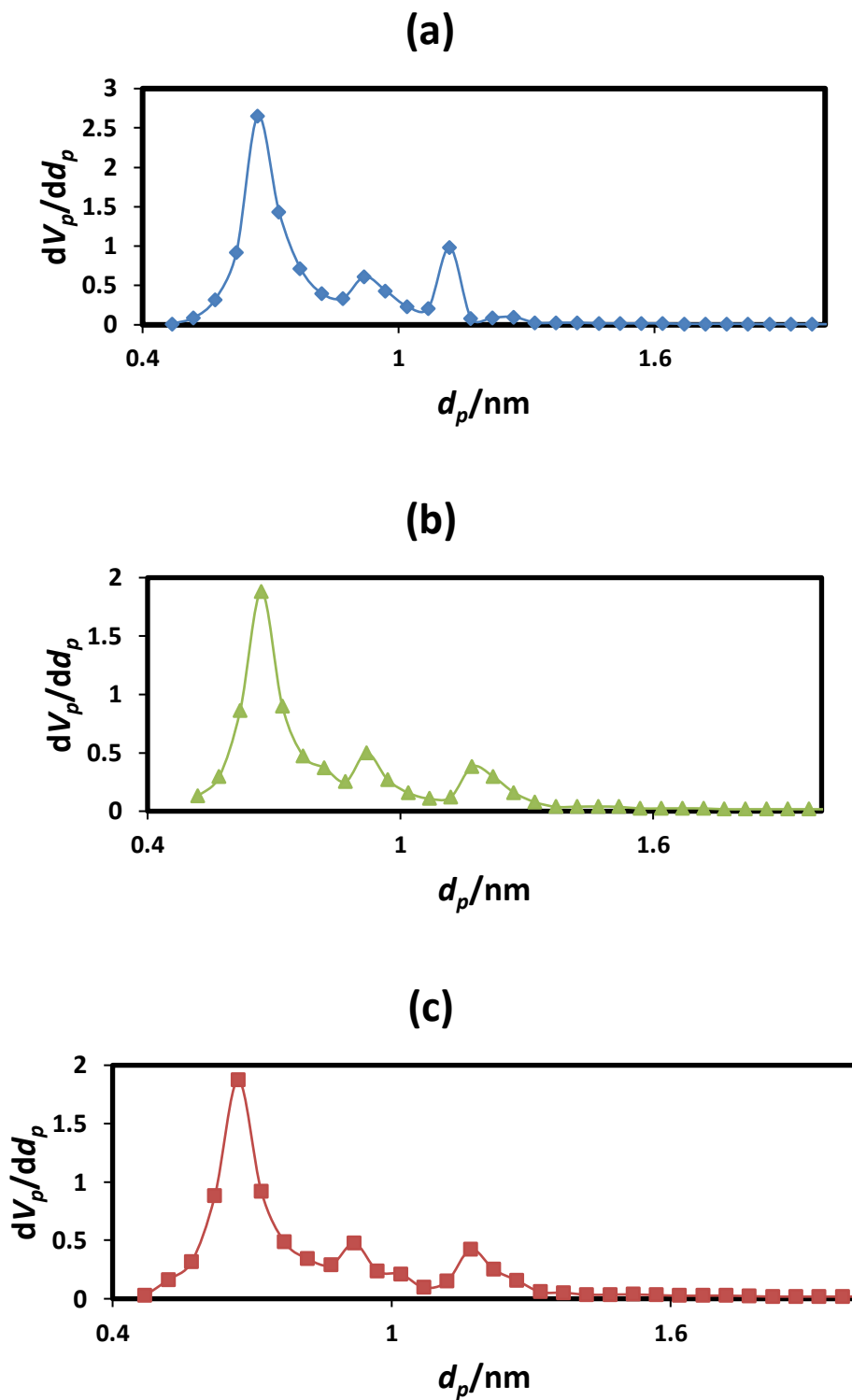


Figure S3. Pore size distribution calculated using the Horvath–Kawazoe method of (a) ZIF-8 NPs, (b) PEG₄₈₀-g-ZIF-8 NPs and (c) PEG₅₀₀₀-g-ZIF-8 NPs.

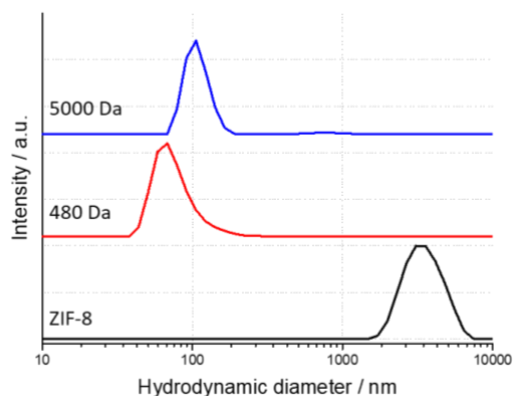
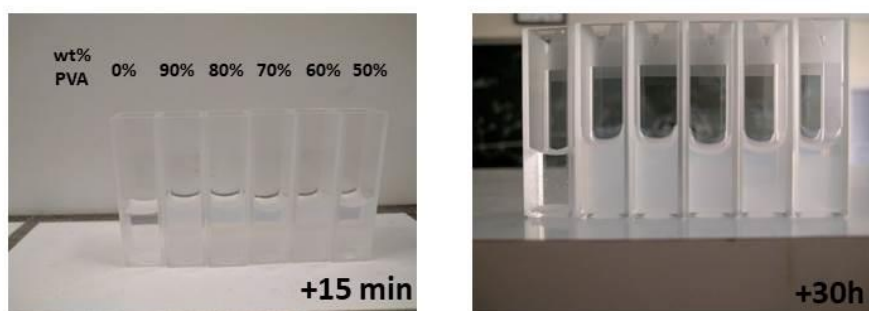
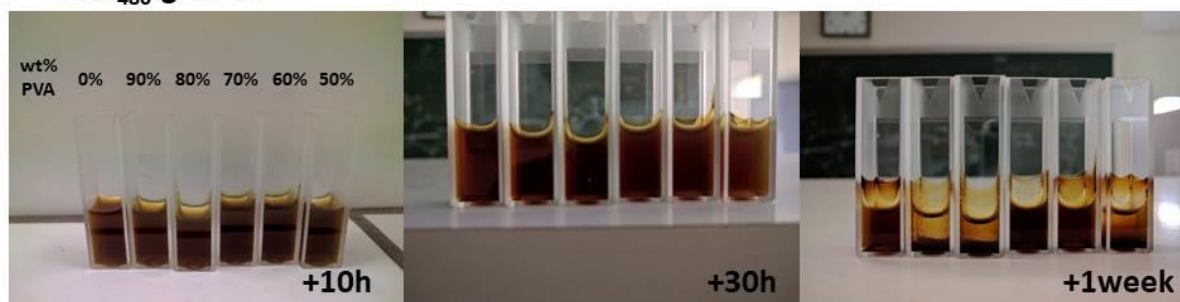


Figure S4: DLS measurements performed on aqueous solutions of ZIF-8 and PEG-g-ZIF-8 NPs at 1 g.L⁻¹. PEG-g-ZIF-8 NPs were prepared with PEG chains of 480 and 5000 Da. Each curve is off-set for better comparison.

Pristine ZIF-8



PEG₄₈₀-g-ZIF-8



PEG₅₀₀₀-g-ZIF-8

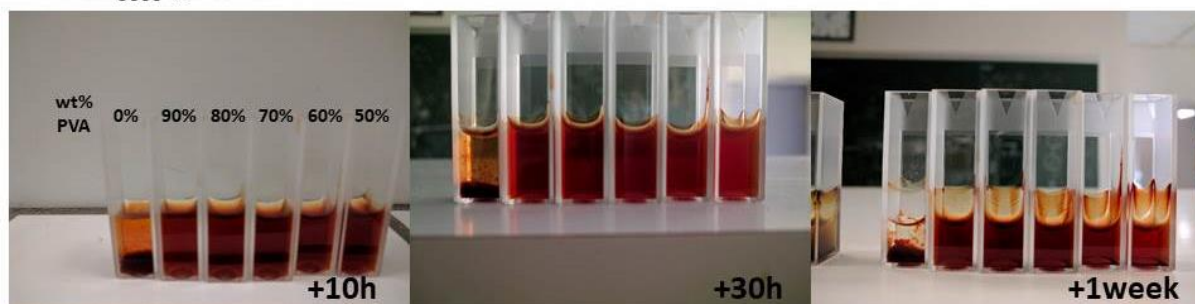


Figure S5. Visual observation of the colloidal stability of ZIF-8 and PEG-g-ZIF-8 NPs at 1 g/L in pure water and aqueous PVA solutions of different PVA content (50-90 wt%).

The long-term colloidal stability of pure ZIF-8 and PEG-g-ZIF-8 NPs in pure water was evaluated by visual observations. The sedimentation of pure ZIF-8 NPs is observed in a short delay of time (< 15 min) while the colloidal solutions of PEG₅₀₀₀-g-ZIF-8 NPs are stable for more than 10h. PEG₄₈₀-g-ZIF-8 NPs are by far the most stable colloids in water since no sedimentation was observed for more than one week. The difference of stability between PEG₅₀₀₀-g-ZIF-8 and PEG₅₀₀₀-g-ZIF-8 NPs colloids in pure water may be imparted by their difference of PEG density (see above). For PEG₅₀₀₀-g-ZIF-8, a density of 100 PEG chains per NP was estimated which is ten times lower than that of PEG₄₈₀-g-ZIF-8 (i. e. 1049 PEG chains per NP).

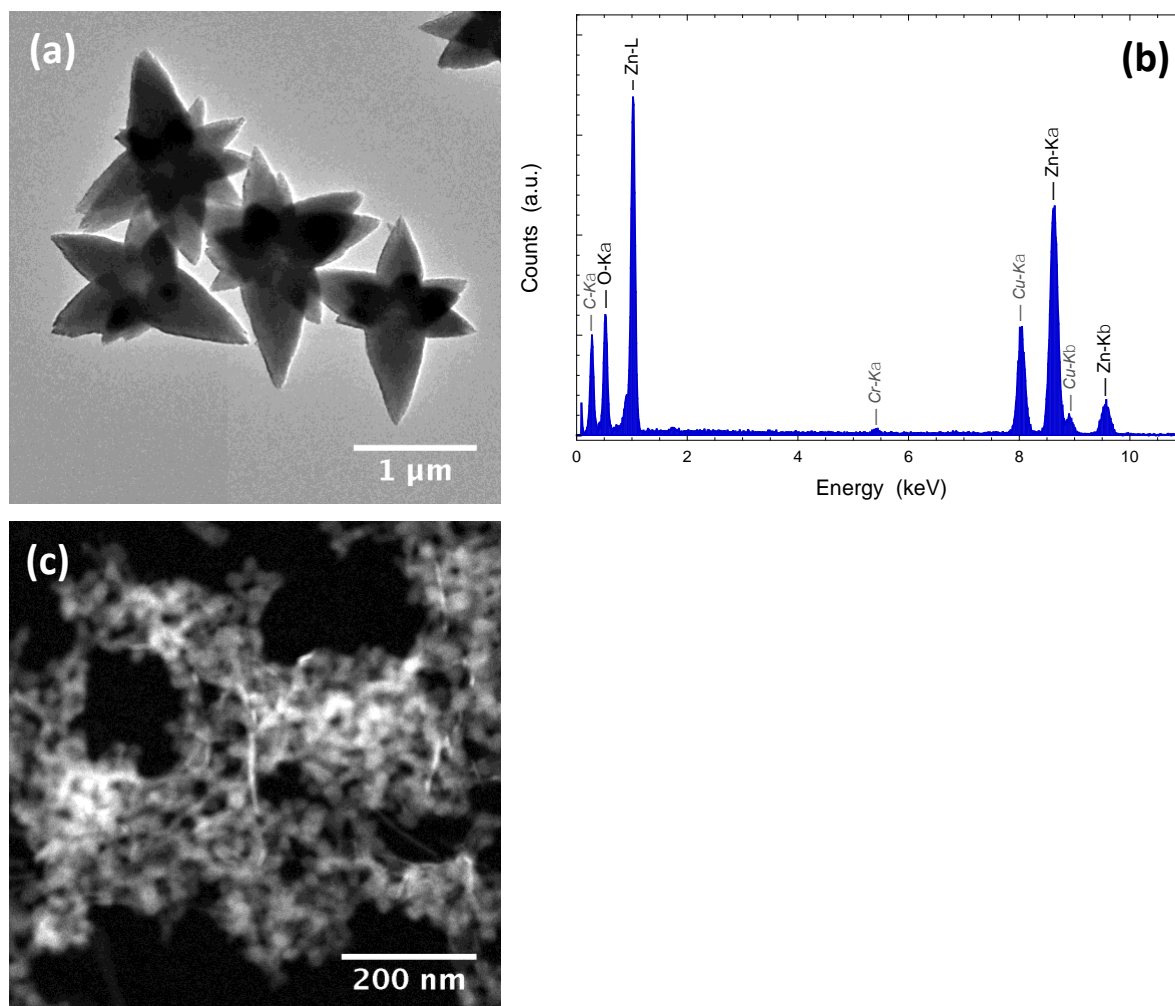


Figure S6. (a) TEM-BF images of particles obtained upon degradation of ZIF-8 NPs after aging in water for 12 days and (b) corresponding XEDS measurement. (c) STEM-HAADF of PEG₅₀₀₀-g-ZIF-8 NPs after ageing in water for 15 days.

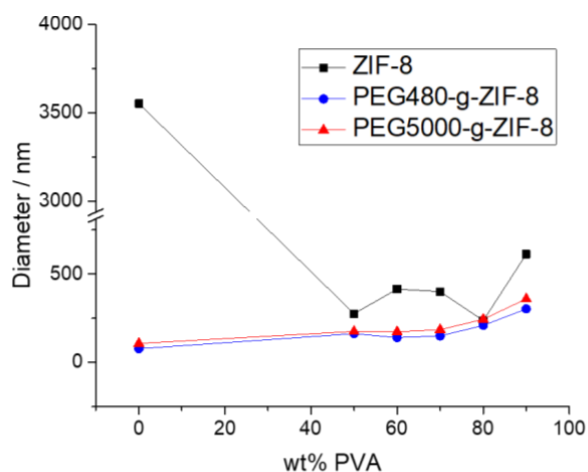


Figure S7. Evolution of the hydrodynamic diameter (measured by DLS) of ZIF-8 and PEG-g-ZIF-8 in water in presence of increasing content of PVA at 1 g.L^{-1} .

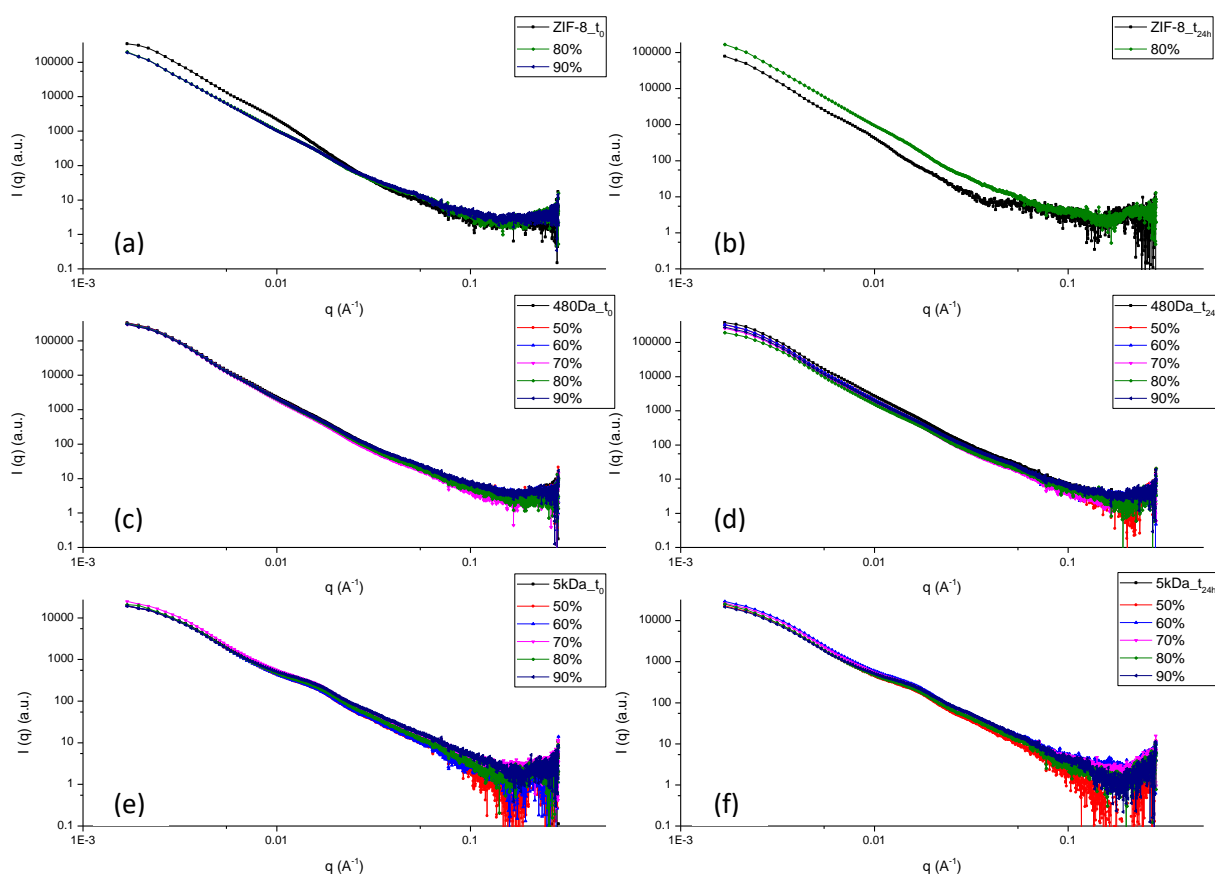


Figure S8. SAXS curves for ZIF-8 (a and b), PEG₄₈₀-g-ZIF-8 (c and d) and PEG₅₀₀₀-g-ZIF-8 (e and f) dispersed in PVA solutions at 1 g.L^{-1} at t_{0h} (a, c, e) and t_{24h} (b, d, f) with PVA content indicated in the insets.

IV-Characterization of Mixed Matrix Membranes based on PVA and ZIF-8 NPs.

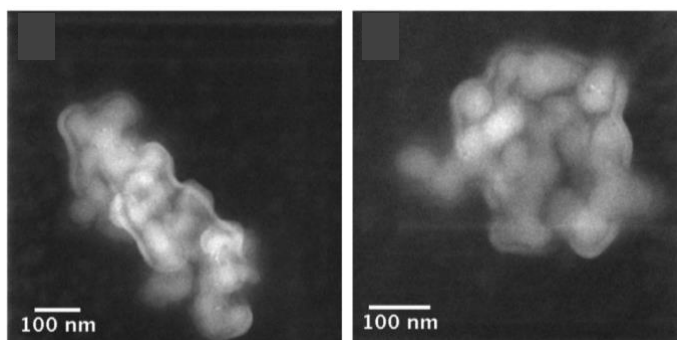


Figure S9. STEM-HAADF images of PEG₅₀₀₀-g-ZIF-8/PVA (90 wt%).

Composite films were prepared through the deposition of PEG₅₀₀₀-g-ZIF-8/PVA (90 wt%) suspensions on carbon grids. Aggregates of a few 100 nm in diameter are observed. A polymer top-layer with a thickness of 7 ± 3 nm is observed at the surface of PEGylated ZIF-8 NPs.

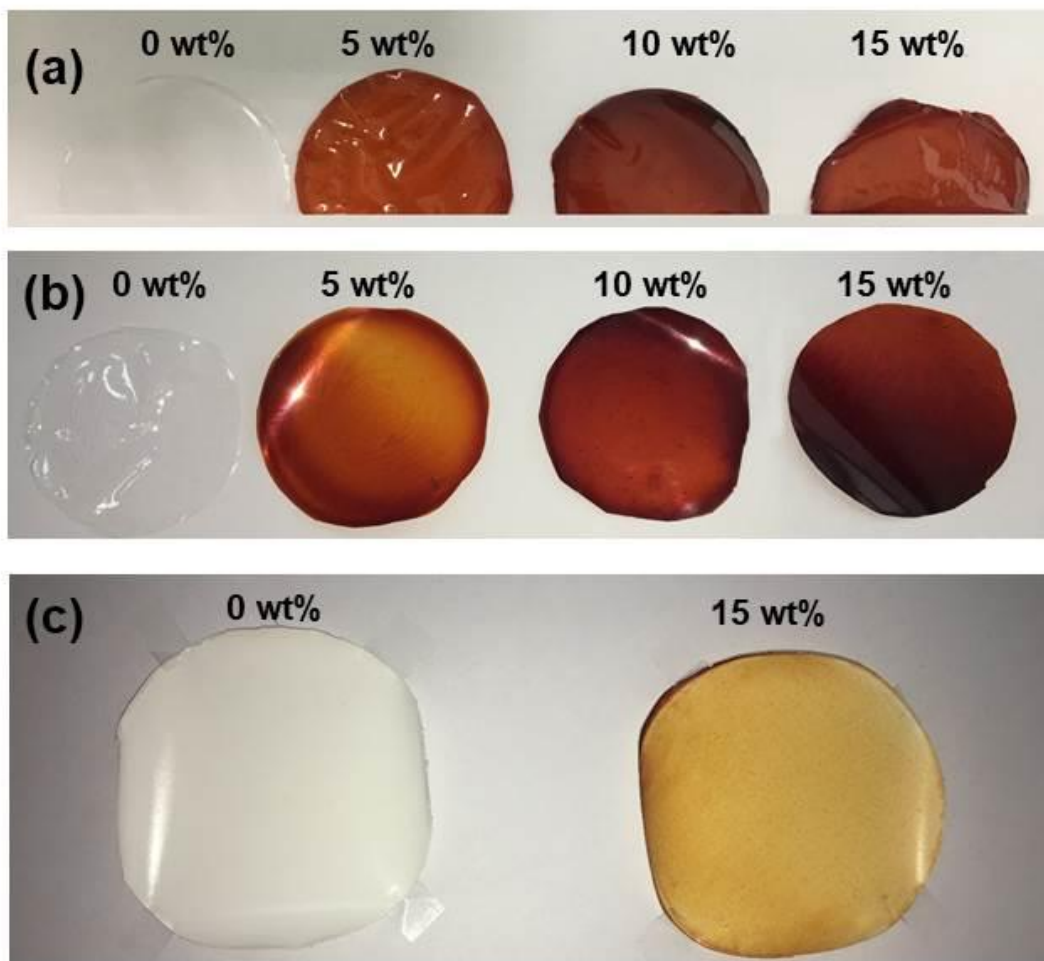


Figure S10. Photographs of dense and supported PVA based MMMs with different content of PEG₅₀₀₀-g-ZIF-8 NPs (a) dense PEG₅₀₀₀-g-ZIF-8/PVA, (b) dense CL-PEG₅₀₀₀-g-ZIF-8/PVA, (c) supported CL-PEG₅₀₀₀-g-ZIF-8/PVA. The amount (in wt%) of PEG₅₀₀₀-g-ZIF-8 NPs is indicated on each photograph.

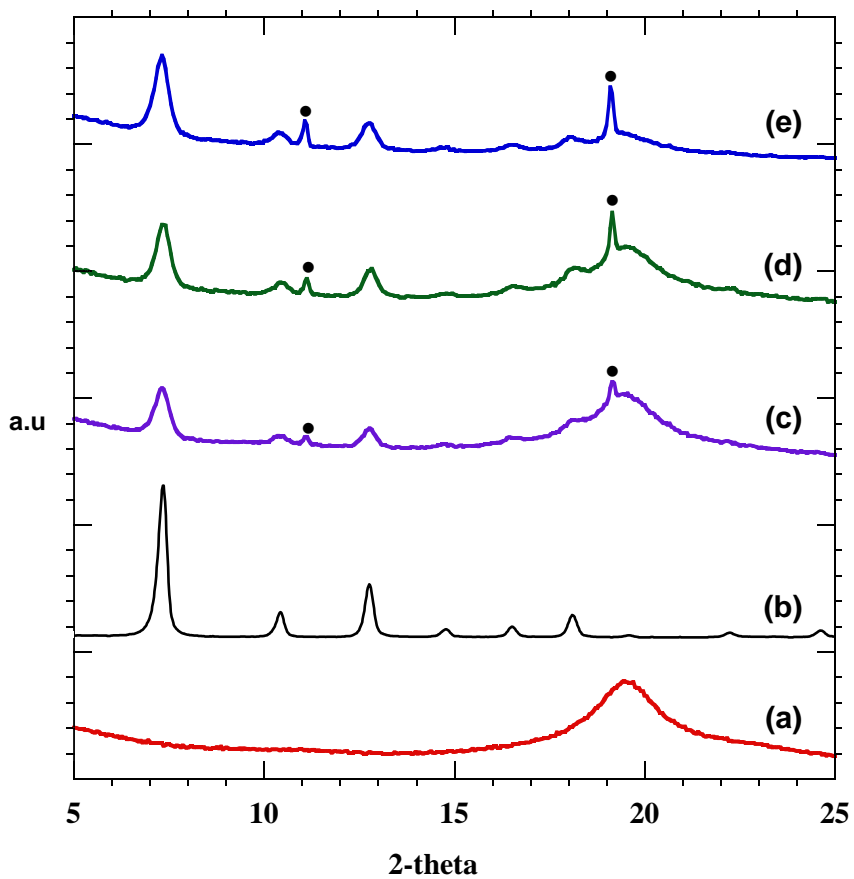


Figure S11. PXRD pattern of (a) pure PVA membrane, (b) PEG₅₀₀₀-g-ZIF-8, (c-e) CL-PEG₅₀₀₀-g-ZIF-8 MMMs with different contents of PEG₅₀₀₀-g-ZIF-8 : c) 5 wt%, d) 10 wt% and e) 15 wt%. The black dots indicated on the pattern correspond to XRD peaks of semi-crystalline PVA, as previously reported.^{7,8}

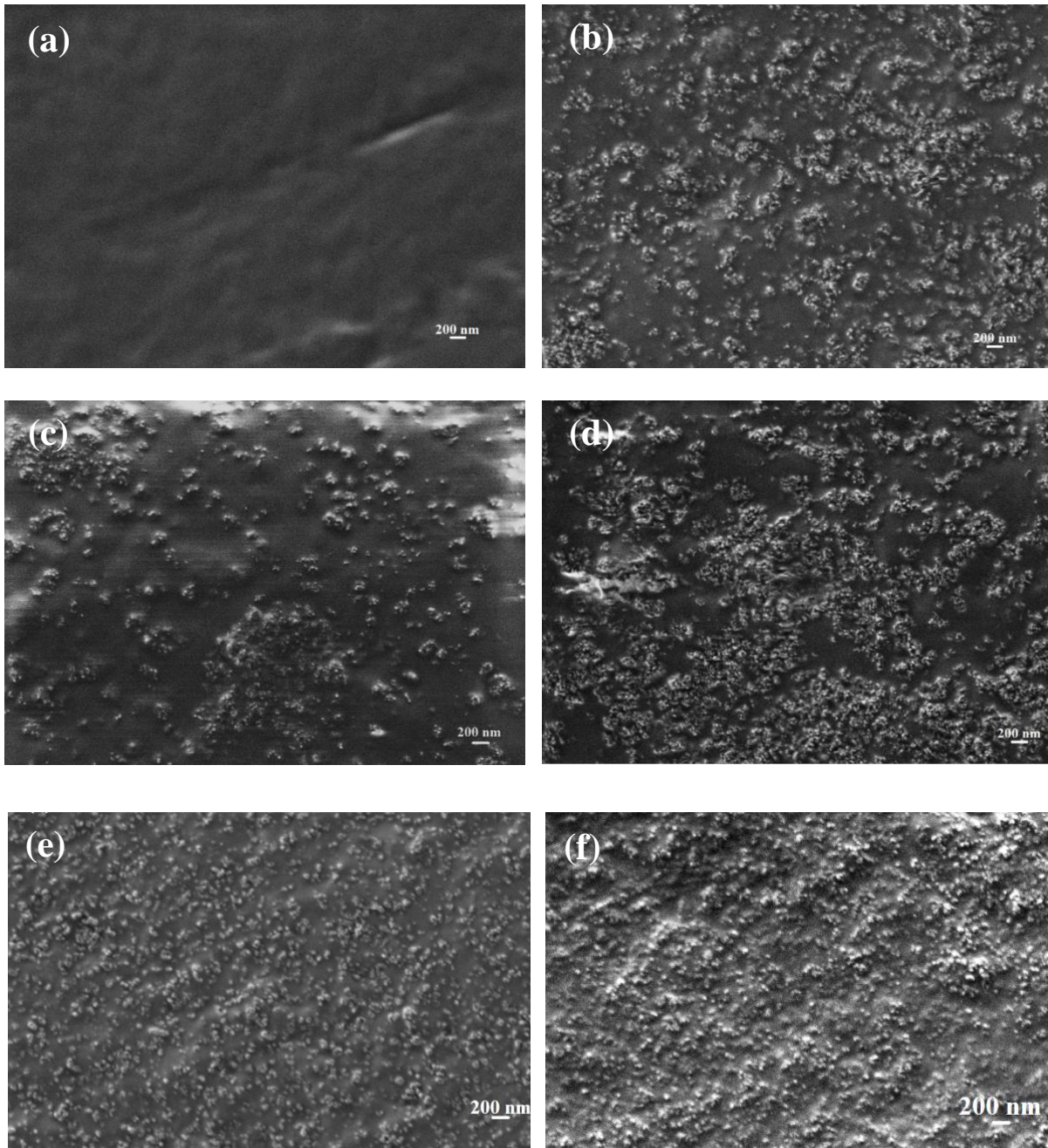


Figure S12. Cross-section SEM images of (a) pure PVA membrane, (b-d) dense PEG₅₀₀₀-g-ZIF-8/PVA MMMs and (e,f) CL-PEG₅₀₀₀-g-ZIF-8/PVA with different contents of PEG₅₀₀₀-g-ZIF-8 NPs: (b) 5 wt%, (c, e) 10 wt% and (d, f) 15 wt%.

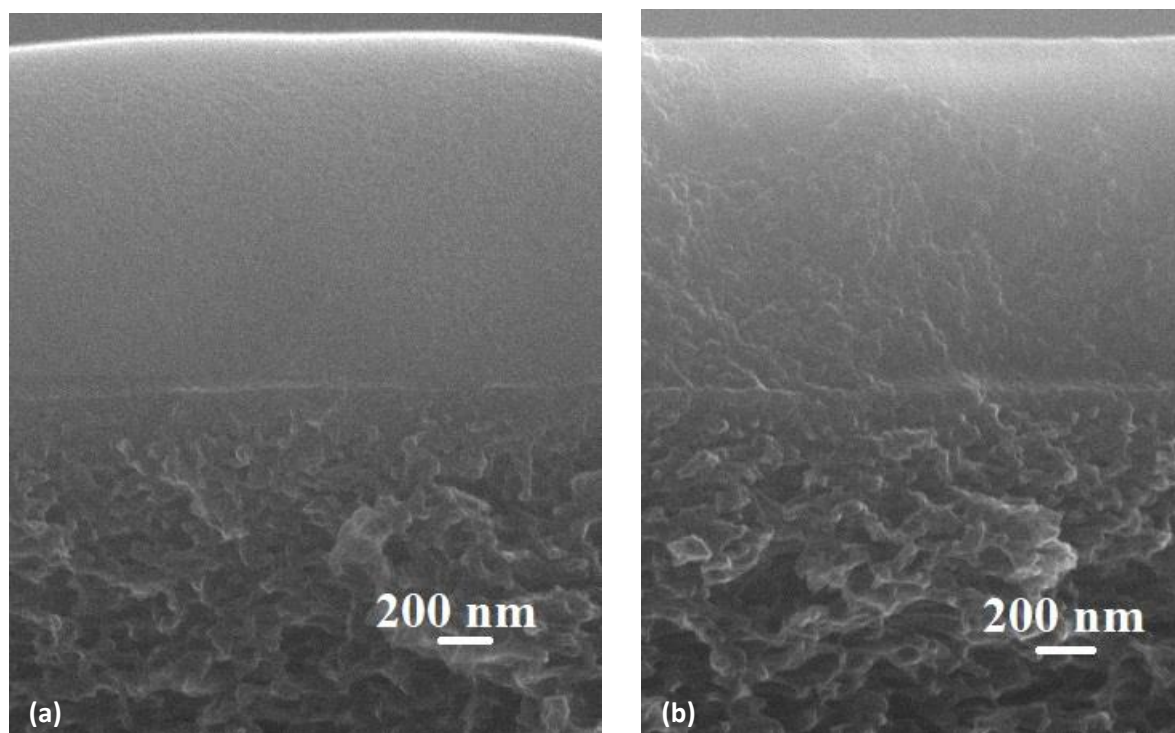


Figure S13. Cross-section SEM images of supported a) CL-PVA and b) CL-PEG₅₀₀₀-g-ZIF-8/PVA MMMs with 15 wt% of PEG₅₀₀₀-g-ZIF-8 NPs. The thin selective layer was deposited at the surface of a UPM-20 support.

Table S2. Water contact angle of CL-PEG₅₀₀₀-g-ZIF-8/PVA MMMs with different content of PEG₅₀₀₀-g-ZIF-8 NPs.

content of PEG ₅₀₀₀ -g-ZIF-8 (wt%)	Water contact angle (°)
0	71
5	93
10	97
15	98

Table S3. Swelling degree of membranes in water (12 wt%) - iPrOH (88 wt%) mixture.

content of PEG ₅₀₀₀ -g-ZIF-8 (wt%)	Swelling degree, %	
	PEG ₅₀₀₀ -g-ZIF-8/PVA	CL-PEG ₅₀₀₀ -g-ZIF-8/PVA
0	18±1	19±1
5	16±1	15±1
10	15±1	14±1
15	13±1	13±1

Table S4. Comparison of transport properties of PVA hybrid membranes for IPA dehydration.

Filler	Feed, water wt%	Temp., °C	Separation factor (β)	Permeation flux, kg/(m ² h)	Reference
Silicalite-1	10	30	2241	0.069	9
SiO ₂ (1 wt%)	10	30	~400	~0.011	10
Ag-modified zeolite (AgNaZ) (~3 wt%)	10	40	5184	0.018	11
MWNTs-PSS (3 wt%) (supported on PAN)	10	30	882	0.168	12
1-n-butyl-3-methylimidazolium chloride (BMIMCl) (9.4 wt%)	10	50	7389	0.0224	13
Clay (clinoptilolite) (10 wt%)	10	30	12848	0.222	14
TiO ₂ (1 wt%)	10	30	∞	0.022	15
TiO ₂ (1 wt%)-polyaniline	10	30	∞	0.025	
ZIF-8 (7.5 wt%)/GA	10	30	91	0.952	2
ZIF-8 (5 wt%)/GA	10	30	132	0.868	
CL-PEG ₅₀₀₀ -g-ZIF-8 (15 wt%) (dense)	12	25	7326	0.034	This study
CL-PEG ₅₀₀₀ -g-ZIF-8 (15 wt%) (supported)	12	25	7326	0.091	This study

V- Molecular modeling.

1. ZIF-8/PVA interface simulations. The ZIF-8/PVA interface was modeled at the atomistic-level by using a methodology developed by some of us integrating quantum- and forcefield-based molecular simulations.¹⁶ First, several model surface slabs for ZIF-8 were built by cutting the bulk MOF with different spatial orientations and minimizing the number of severed bonds. The Density Functional Theory (DFT) optimized {011} surface was selected among those investigated for having the lowest energy, and a flexible model of it was considered for the subsequent molecular dynamics (MD) runs.¹⁷ This surface features alternating imidazolate and OH groups capping the most external Zn atoms, as illustrated in Figure S14.

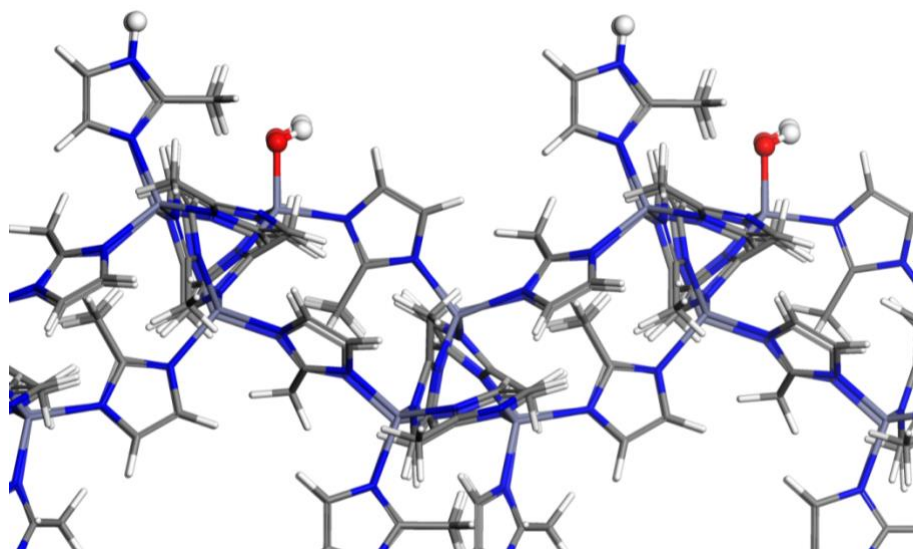


Figure S14. Scheme of the ZIF-8 {011} surface. Color code: O (red), C (grey), H (white), N (blue), Zn (purple). Surface terminations are highlighted by means of a different atom representation.

As a second step, PVA was modelled as a polydisperse mixture of 7 chains between 50 and 300 monomers, constructed using *polymatic*,¹⁸ and *lammgs*.¹⁹ This model contains a total of 7133 atoms considering chain terminations, and it is large enough to avoid the interaction of the two external surfaces of the MOF slab when they are combined. The force field of the polymer consists of bonded and non-bonded contributions. The bonded contributions were modeled as harmonic potentials for stretchings and bendings, and cosine-based functions for dihedral angles. Non-bonded interactions were treated as a summation of 12-6 Lennard-Jones (LJ) and coulombic potentials. All parameters were taken from the CHARMM force field.²⁰ Crossed interactions were computed by using the Lorentz-Berthelot mixing rules.²¹ The cutoff was set to 12 Å. A scheme of the monomer is presented in Figure S15 and the non-bonded

parameters/charges are gathered in Table S5. The polymer chains were terminated by adding CH₃ groups at both ends, consisting of CT3 carbons and HA hydrogens. As such, charge neutrality is preserved.

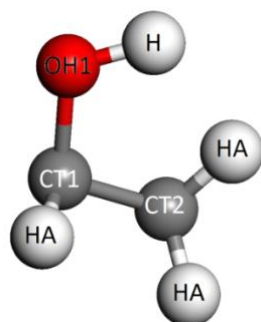


Figure S15. Scheme of the PVA monomer model. Color code as in Figure S14.

Table S5. Atom types, LJ parameters and charges for the PVA model. CT3 are the terminal carbons.

Atom type	ϵ_{ii} (kcal/mol)	σ_{ii} (Å)	q_i (e)
CT1	0.0200	4.05	+0.14
CT2	0.0550	3.88	-0.18
CT3	0.0800	3.67	-0.27
HA	0.0220	2.35	+0.09
OH1	0.1521	3.15	-0.66
H	0.0460	0.40	+0.43

Finally, the interface was built by applying the methodology in Ref. 13. The modeled MOF and polymer species were first equilibrated and then combined. Seven cycles of three molecular dynamics simulations were performed, each of them consisted of two simulations in the NVT ensemble and one in an ensemble with constant number of particles, temperature and pressure component in the direction perpendicular to the slab (NP_nT with n=z). The first simulation in each cycle was conducted at T = 600 K, while for the others temperature was set to 300 K. The pressure was increased in the first three cycles until reaching 1 kbar and then decreased up to ambient pressure in the remaining 4 cycles. The values for temperature and pressure were selected by applying a similar procedure to the equilibration of the bulk polymer and checking that the correct density was obtained. Ten statistically independent simulations were performed. After these cycles, data were collected from molecular dynamics runs, each one lasting 10 ns, with a time step of 1 fs. The equilibration, interface generation and production runs procedures

were the same as previously applied to the ZIF-8/PIM-1 and ZIF-8/PIM-EA-TB systems.^{16,22} Berendsen thermostat and a modified version of the Berendsen barostat that allows for a compression only in the direction perpendicular to the surface were used, with relaxation times of 0.1 and 0.5 ps respectively.²³ For the interface generation and production simulations a modified version of DLPOLY classic has been used.²⁴

In complement to this, the interactions between PVA and the MOF surface were also investigated at DFT-level using a cluster approach. Two clusters containing 10 PVA monomers were extracted from the MD runs and used for further DFT single-point energy calculations. The ZIF-8 cluster is depicted in Figure S16. It consists of two surface Zn atoms, one of them fully coordinated with four imidazolate moieties and the other with one OH and three imidazolate moieties. Two hydrogen atoms were added to the terminal nitrogen atoms of the ZIF-8 cluster as shown in the Figure, in order to cure the dangling bonds. The binding energies were estimated, in order to analyze the strength of PVA/ZIF-8 interactions, using the following equation:

$$\Delta E = E_{PVA/MOF} - E_{PVA} - E_{MOF}$$

where $E_{PVA/MOF}$, E_{PVA} and E_{MOF} are, respectively, the single-point energies of the PVA/ZIF-8 cluster, the PVA chain and the ZIF-8 cluster in a cubic cell of 30 Å.

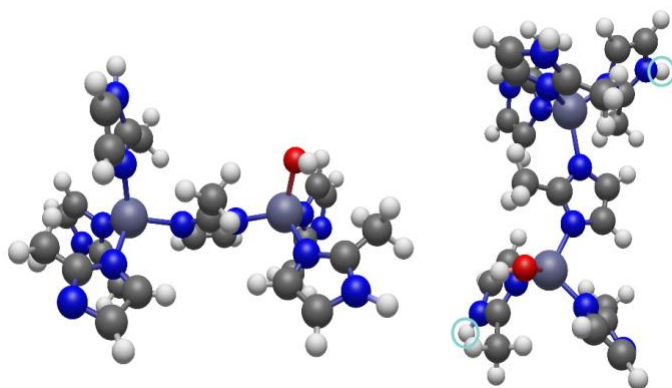


Figure S16. Representation of the ZIF-8 cluster. The hydrogen atoms bonded to the terminal nitrogen atoms are marked by the light blue circles. Color code as in Figure S14.

The single-point energy calculations were performed using the Quantum Espresso package,²⁵ which implements DFT under periodic boundary conditions with plane wave functions as a basis set.^{26,27} The ion cores were described by Vanderbilt ultrasoft pseudopotentials,²⁸ the Kohn-Sham one-electron states were expanded in a planewave basis set with a kinetic cutoff energy of 30 Ry (300 Ry for the density cutoff) and the GGA/PBE functional was used.²⁹ All calculations were performed at the Γ -point. To further assess the compatibility between PVA and the PEGylated-ZIF-8 surface, we modeled the PVA/PEG interface using a similar protocol

to that described above for the ZIF-8/PVA interface. This PVA/PEG interface is taken as representative of the interactions between PVA and the PEGylated particles. PEG and PVA were both represented as flexible polymer chains built separately with the *polymatic* code¹⁸ using the DREIDING force field potential energy parameters.³⁰ The two polymers were brought together in the same simulation box, and an equilibration consisting of 21 MD steps in the NVT and NPT ensembles as proposed by Hofmann *et al.*³¹ was performed, followed by a microscopic description of the composite system obtained from five independent NVT trajectories of 10 ns each.

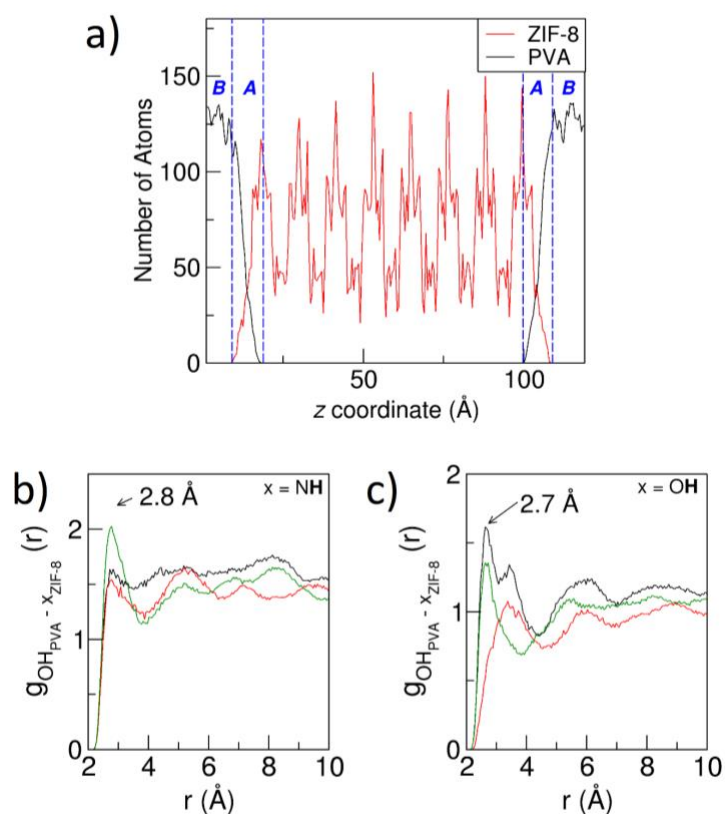


Figure S17. (a) Atomic density profile of PVA and ZIF-8 along the direction perpendicular to the MOF surface slab. (b),(c) Site-site radial distribution functions between the O atom of the OH group present in PVA and the H atom of the surface terminating $-NH$ and $-OH$ groups in ZIF-8. The different plots correspond to 3 independent MD trajectories.

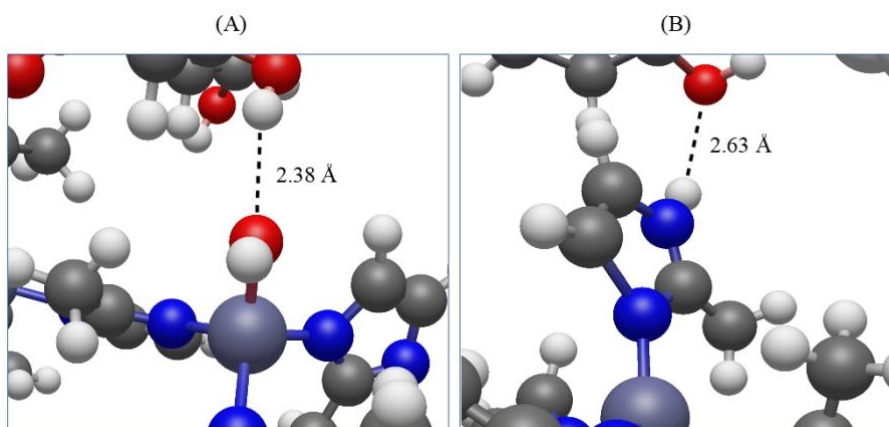


Figure S18. Illustration of the main interactions between PVA and ZIF-8: (A) –OH (PVA) and –OH (ZIF-8) and (B) –OH(PVA) and –NH(ZIF-8). Zn, carbon, nitrogen, oxygen and hydrogen atoms are depicted in purple, grey, blue, red and white respectively.

2. PEG/PVA interface simulations. PVA and PEG were modeled as a polydisperse mixture of 23 and 8 chains respectively, between 10 and 250 monomers, constructed using *polymatic*,¹⁸ and *lammmps*.¹⁹ The force field of the polymers consists of bonded and non-bonded contributions. All parameters were taken from the DREIDING force field.³⁰ Crossed interactions were computed by using the Lorentz-Berthelot mixing rules.²¹ The cutoff was set to 12 Å. The same capping as before was adopted for the PVA, while the terminations of PEG were capped with –H and –OH groups. Tables S6 and S7 summarize the non-bonded parameters of PVA and PEG, respectively. Figure S19 illustrates the PEG monomer.

Table S6. Atom types, Lennard-Jones (LJ) parameters and charges for the PVA model used for building the PEG/PVA interface. CT3 are the terminal carbons. See reference labels in Figure S19.

Atom type	ϵ_{ii} (kcal/mol)	σ_{ii} (Å)	q_i (e)
CT1	0.095	4.35	+0.29
CT2	0.095	4.35	-0.44
CT3	0.095	4.35	-0.39
HA	0.010	3.59	+0.13
OH1	0.215	3.94	-0.62
H	0.000	2.69	+0.38

Table S7. Atom types, LJ parameters and charges for the PEG model used for building the PEG/PVA interface. OH and HO are the terminal oxygen and hydrogen atoms respectively.

Atom type	ϵ_{ii} (kcal/mol)	σ_{ii} (Å)	q_i (e)
C	0.095	4.35	+0.2520
H	0.010	3.59	+0.0205
O	0.215	3.94	-0.5860
OH	0.215	3.94	-0.384
HO	0.000	2.69	+0.192

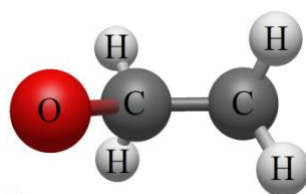


Figure. S19. Scheme of the PEG monomer model. Color code as in Figure S14.

VI-References

- (1) Tsai, C.-W.; Langner, E. H. G. The Effect of Synthesis Temperature on the Particle Size of Nano-ZIF-8. *Microporous Mesoporous Mater.* **2016**, *221*, 8–13, DOI 10.1016/j.micromeso.2015.08.041.
- (2) Amirilargani, M.; Sadatnia, B. Poly(vinyl alcohol)/Zeolitic Imidazolate Frameworks (ZIF-8) Mixed Matrix Membranes for Pervaporation Dehydration of Isopropanol, *J. Memb. Sci.* **2014**, *469*, 1–10, DOI 10.1016/j.memsci.2014.06.034.
- (3) Dmitrenko, M. E.; Penkova, A.V.; Kuzminova, A. I.; Morshed, M.; Larionov, M. I.; Alem, H.; Zolotarev, A. A; Ermakov, S. S.; Roizard, D. Investigation of New Modification Strategies for PVA Membranes to Improve Their Dehydration Properties by Pervaporation, *Appl. Surf. Sci.* **2018**, *450*, 527–537, DOI 10.1016/j.apsusc.2018.04.169
- (4) Baker, R.W. ; Wijmans, J. G. ; Huang, Y. Permeability, Permeance and Selectivity: A Preferred Way of Reporting Pervaporation Performance Data, *J. Memb. Sci.* **2010**, *348*, 346–352, DOI 10.1016/j.memsci.2009.11.022.

-
- (5) Auguste, D. T.; Armes, S. P.; Brzezinska, K. R.; Deming, T. J.; Kohn, J.; Prud'homme, R. K. pH Triggered Release of Protective Poly(Ethylene Glycol)-b-Polycation Copolymers from Liposomes. *Biomaterials* **2006**, *27*, 2599–2608, DOI 10.1016/j.biomaterials.2005.08.036.
- (6) Xu, Q.; Ensign, L. M.; Boylan, N. J.; Schön, A.; Gong, X.; Yang, J.-C.; Lamb, N. W.; Cai, S.; Freire, E.; Hanes, J. Impact of Surface Polyethylene Glycol (PEG) Density on Biodegradable Nanoparticle Transport in Mucus ex Vivo and Distribution in Vivo. *ACS Nano* **2015**, *9*, 9217-9227, 10.1021/acs.nano.5b03876.
- (7) Assender, H. E.; Windle, A. H. Crystallinity in Poly(vinyl alcohol).1. An X-ray Diffraction Study of Atactic PVOH. *Polymer* **1998**, *39*, 4295-4302.
- (8) Penkova, A. V.; Acquah, S. F. A.; Sokolova, M. P.; Dmitrenko, M. E.; Toikka, A. M. Polyvinylalcohol Membranes Modified by Low-hydroxylated Fullerenol C₆₀(OH)₁₂. *J. Membr. Sci.* **2015**, *491*, 22–27, DOI 10.1016/j.memsci.2015.05.011.
- (9) Adoor, S. G.; Prathab, B.; Manjeshwar, L. S.; Aminabhavi, T. M. Mixed Matrix Membranes of Sodium Alginate and Poly(vinyl alcohol) for Pervaporation Dehydration of Isopropanol at Different Temperatures. *Polymer* **2007**, *48*, 5417-5430, DOI 10.1016/j.polymer.2007.06.064.
- (10) Arif, Z.; Sethy, N. K. Mishra, P. K.; Upadhyay, S. N.; Verma, B. Investigating the Influence of Sol Gel Derived PVA/SiO₂ Nano Composite Membrane on Pervaporation Separation of Azeotropic mixture I. Effect of Operating Condition. *J. Porous Mater.* **2018**, *25*, 1203-1211, DOI 10.1007/s10934-017-0530-y.
- (11) Kwon, Y. S.; Chaudhari, S.; Kim, C. E.; Son, D. H.; Park, J. H.; Moon, M. J.; Shon, M.Y.; Park, Y.; Nam, S. E. Ag-exchanged NaY Zeolite Introduced Polyvinyl Alcohol/Polyacrylic acid Mixed Matrix Membrane for Pervaporation Separation of Water/Isopropanol Mixture. *RSC Adv.* **2018**, *8*, 20669–20678, DOI 10.1039/c8ra03474e.
- (12) Amirilargani, M.; Ahmadzadeh Tofighy, M.; Mohammadi, T.; Sadatnia, B. Novel Poly(vinyl alcohol)/Multiwalled Carbon Nanotube Nanocomposite Membranes for Pervaporation Dehydration of Isopropanol: Poly(sodium 4-styrenesulfonate) as a Functionalization Agent. *Ind. Eng. Chem. Res.* **2014**, *53*, 12819–12829, DOI 10.1021/ie501929m.
- (13) Thorat, G. B.; Gupta, S.; Murthy, Z.V. P. Synthesis, Characterization and Application of PVA/Ionic Liquid Mixed Matrix Membranes for Pervaporation Dehydration of Isopropanol. *Chin. J. Chem. Eng.* **2017**, *25*, 1402-1411, 10.1016/j.cjche.2017.02.011.

-
- (14) Ravindra, S.; Rajinikanth, V.; Mulaba-Bafubiandi, A. F.; Vallabhapurapu, V. S. Performance Enhancement of the Poly (vinyl alcohol) (PVA) by Activated Natural Clay Clinoptilolite for Pervaporation Separation of Aqueous–Organic Mixtures. *Desalin. Water Treat.* **2015**, *57*, 4920-4934, DOI 10.1080/19443994.2014.999131.
- (15) Sairam, M. ; Patil, M. B.; Veerapur, R. S.; Patil, S. A.; Aminabhavi, T. M. Novel Dense Poly(vinyl alcohol)–TiO₂ Mixed Matrix Membranes for Pervaporation Separation of Water–Isopropanol Mixtures at 30 °C. *J. Memb. Sci.* **2006**, *281*, 95–102, DOI 10.1016/j.memsci.2006.03.022.
- (16) Semino R.; Ramsahye, N. A.; Ghoufi, A.; Maurin G. Microscopic Model of the Metal-Organic Framework/Polymer Interface: A First Step toward Understanding the Compatibility in Mixed Matrix Membranes. *ACS Appl. Mater. Interfaces* **2016**, *8*, 809-819, DOI 10.1021/acsami.5b10150.
- (17) Zheng, B.; Sant, M.; Demontis, P.; Suffritti, G. B. Force Field for Molecular Dynamics Computations in Flexible ZIF-8 Framework. *J. Chem. Phys. C* **2012**, *116*, 933-938, DOI 10.1021/jp209463a.
- (18) Abbott, L. J.; Hart, K. E.; Colina, C. M. Polymatic: A Generalized Simulated Polymerization Algorithm for Amorphous Polymers. *Theor. Chem. Acc.* **2013**, *132*, 1334, DOI 10.1007/s00214-013-1334-z.
- (19) Plimpton, S. Fast Parallel Algorithms for Short-Range Molecular Dynamics. *J. Comput. Phys.* **1995**, *117*, 1-19, DOI 10.1006/jcph.1995.1039.
- (20) MacKerell, A. D.; Bashford, D.; Bellott, M.; Dunbrack, R. L.; Evanseck, J. D.; Field, M. J.; Fischer, M. J.; Gao, J.; Guo, H.; Ha, S.; Joseph-McCarthy, D.; Kuchnir, L.; Kuczera, K.; Lau, F. T. K.; Mattos, C.; Michnick, S.; Ngo, T.; Nguyen, D. T.; Prodhom, B.; Reiher, W. E.; Roux, B.; Schlenkrich, M.; Smith, J. C.; Stote, R.; Straub, J.; Watanabe, M.; Wiórkiewicz-Kuczera, J.; Yin, D.; M. Karplus. All-Atom Empirical Potential for Molecular Modeling and Dynamics Studies of Proteins. *J. Phys. Chem. B* **1998**, *102*, 3586-3616, DOI 10.1021/jp973084f.
- (21) M. P. Allen and D. J. Tildesley, *Computer Simulation of Liquids*, Oxford Science Publications: Oxford, 1989.
- (22) Benzaqui, M.; Semino, R.; Menguy, N.; Carn, F.; Kundu, T.; Guigner, J.-M.; McKeown, N. B.; Msayib, K. J.; Carta, M.; Malpass-Evans, R.; Le Guillouzer, C.; Clet, G.; Ramsahye, N. A.; Serre, C.; Maurin, G.; Steunou, N. Toward an Understanding of the Microstructure and Interfacial Properties of PIMs/ZIF-8 Mixed Matrix Membranes. *ACS Appl. Mater. Interfaces* **2016**, *8*, 27311–27321, DOI 10.1021/acsami.6b08954.
- (23) Berendsen, H. J. C.; Postma, J. P. M.; van Gunsteren, W. F.; DiNola, A.; Haak, J. R. Molecular Dynamics with Coupling to an External Bath. *J. Chem. Phys.* 1984, **81**, 3684, DOI 10.1063/1.448118.
- (24) Todorov, I. T.; Smith, W.; Trachenko, K.; Dove, M. T. DL_POLY_3: New Dimensions in Molecular Dynamics Simulations via Massive Parallelism. *J. Mater. Chem.* **2006**, *16*, 1911-1918, DOI 10.1039/B517931A.

-
- (25) Giannozzi, P.; Baroni, S.; Bonini, N.; Calandra, M.; Car, R.; Cavazzoni, C.; Ceresoli, D.; Chiarotti, G. L.; Cococcioni, M.; Dabo, I. *et al.* Quantum ESPRESSO: a Modular and Open-source Software Project for Quantum Simulations of Materials. *J. Phys.: Condens. Matter* **2009**, *21*, 395502, DOI 10.1088/0953-8984/21/39/395502.
- (26) Hohenberg, P.; Kohn, W. Inhomogeneous Electron Gas. *Phys. Rev.* **1964**, *136*, B864, DOI 10.1103/PhysRev.136.B864.
- (27) Kohn, W.; Sham, L. J. Self-Consistent Equations Including Exchange and Correlation Effects. *Phys. Rev.* **1965**, *140*, A1133, DOI 10.1103/PhysRev.140.A1133.
- (28) Vanderbilt, D. Soft Self-Consistent Pseudopotentials in a Generalized Eigenvalue Formalism. *Phys. Rev. B* **1990**, *41*, 7892(R), DOI 10.1103/PhysRevB.41.7892.
- (29) Perdew, J. P.; Burke, K.; Ernzerhof, M. Generalized Gradient Approximation Made Simple. *Phys. Rev Lett.* **1996**, *77*, 3865-3868, DOI 10.1103/PhysRevLett.77.3865.
- (30) Mayo, S. L.; Olafson, B. D.; Goddard, W. A. DREIDING: a Generic Force Field for Molecular Simulations. *J. Phys. Chem.* **1990**, *94*, 8897-8909, DOI 10.1021/j100389a010.
- (31) Hofmann, D.; Fritz, L.; Ulbrich, J.; Schepers, C.; Böhning, M. Detailed-Atomistic Molecular Modeling of Small Molecule Diffusion and Solution Processes in Polymeric Membrane Materials. *Macromol. Theory Simul.* **2000**, *9*, 293-327, DOI 10.1002/1521-3919(20000701)9:6<293::AID-MATS293>3.0.CO;2-1.